Inorganic Chemistry

ARTICLE

pubs.acs.org/IC

Redox Potentials of Oxoiron(IV) Porphyrin π-Cation Radical Complexes: Participation of Electron Transfer Process in Oxygenation Reactions

Akihiro Takahashi, Takuya Kurahashi, and Hiroshi Fujii*

Institute for Molecular Science and Okazaki Institute for Integrative Bioscience, National Institutes of Natural Sciences, Myodaiji, Okazaki 444-8787, Japan, and Department of Functional Molecular Science, The Graduate University for Advanced Studies, Myodaiji, Okazaki 444-8787, Japan

Supporting Information

ABSTRACT: The oxoiron(IV) porphyrin π-cation radical complex (compound I) has been identified as the key reactive intermediate of several heme enzymes and synthetic heme complexes. The redox properties of this reactive species are not yet well understood. Here, we report the results of a systematic study of the electrochemistry of oxoiron(IV) porphyrin π-cation radical complexes with various porphyrin structures and axial ligands in organic solvents at low temperatures. The cyclic voltammogram of (TMP)$Fe^{IV}O$, (TMP = 5,10,15,20-tetramesitylporphyrinate), exhibits two quasi-reversible redox waves at $E_{1/2}$ = 0.88 and 1.18 V vs SCE in dichloromethane at −60 °C. Absorption spectral measurements for electrochemical oxidation at controlled potential clearly indicated that the first redox wave results from the (TMP)$Fe^{IV}O$/[(TMP$^{+\bullet}$)$Fe^{IV}O$]$^+$ couple. The redox potential for the (TMP)$Fe^{IV}O$/[(TMP$^{+\bullet}$)$Fe^{IV}O$]$^+$ couple undergoes a positive shift upon coordination of an anionic axial ligand but a negative shift upon coordination of a neutral axial ligand (imidazole). The negative shifts of the redox potential for the imidazole complexes are contrary to their high oxygenation activity. On the other hand, the electron-withdrawing effect of the meso-substituent shifts the redox potential in a positive direction. Comparison of the measured redox potentials and reaction rate constants for epoxidation of cyclooctene and demethylation of *N*,*N*-dimethylanilines enable us to discuss the details of the electron transfer process from substrates to the oxoiron(IV) porphyrin π-cation radical complex in the oxygenation mechanisms.

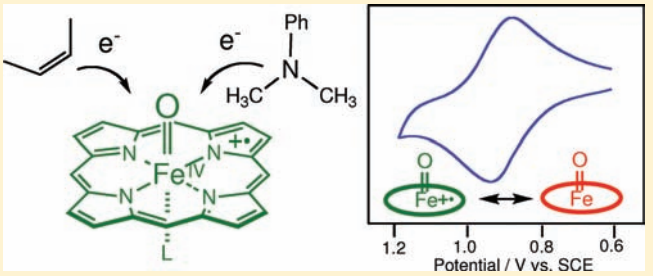

INTRODUCTION

The oxoiron(IV) porphyrin π-cation radical species, which is an oxidation state two-electron equiv higher than the resting state, is a reactive intermediate known as compound I of heme-containing peroxidases, catalases, and cytochrome P450.[1−5] Peroxidases catalyze one-electron oxidations of amines, phenols, and other aromatic substrates with compound I while catalases oxidize hydrogen peroxide to oxygen molecule with compound I.[1,2] Compound I of cytochrome P450 can hydroxylate saturated hydrocarbons.[3,4] Because of its biological significance and extremely high reactivity, compound I has also received much attention with respect to biomimetic monooxygenation catalysis with synthetic heme complexes. After Groves et al. prepared the first example of a synthetic oxoiron(IV) porphyrin π-cation radical structure using an iron 5,10,15,20-tetramesitylporphyrin (TMP) complex,[6] various types of oxidation reactions of compound I, such as epoxidations of olefins,[6−11] hydroxylations of hydrocarbons,[9,11,12] sulfoxidations of sulfides,[13] and demethylations of anisoles and *N*,*N*-dimethylanilines,[14] were studied. The reaction mechanisms of these oxidation reactions have been studied with chemical and theoretical methods but remain the subject of debate.[12−22]

Because compound I is reduced to a ferric heme complex in the process of carrying out its oxidation reactions, the reactions of compound I with substrates accompany electron transfer from the substrates to compound I. Therefore, characterization of the redox potential of compound I has been thought to be a key to gaining an understanding of its reaction mechanism. Compound I and compound II, which is one-electron reduced form of compound I, of certain peroxidases are relatively stable at room temperature. The redox potentials of compound I/compound II of these peroxidases were measured using chemical and electrochemical methods.[23−30] The redox potentials for compound I/compound II were reported to be in the range of 900−1150 mV versus NHE (660−910 mV vs SCE). These redox potentials were unexpectedly lower than anticipated for species with such high oxidizing activity toward various organic substrates. However, the electrochemistry of the oxoiron(IV) porphyrin π-cation radical complex in organic solvent has not been well studied because of its instability at room temperature. Balch et al. reported that the oxoiron(IV) TMP complex,

Received: December 24, 2010
Published: June 29, 2011

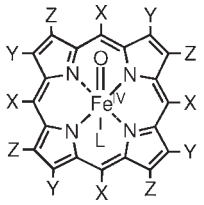

	X	Y	Z
TMP	Me_3-C_6H_2	H	H
TDCP	2,6-$Cl_2C_6H_3$	H	H
TPFP	C_6F_5	H	H
TMTMP	H	Me_3-C_6H_2	Me

Figure 1. Structures of the oxoiron(IV) porphyrin complexes used in this study.

(TMP)$Fe^{IV}O$, was oxidized to its π-cation radical complex, $[(TMP^{+\bullet})Fe^{IV}O]^+$ with an iron(III) porphyrin π-cation radical species at −80 °C.[31] This suggests that the redox potential for the (TMP)$Fe^{IV}O/[(TMP^{+\bullet})Fe^{IV}O]^+$ couple was lower than that of $[(TMP)Fe^{III}]^+/[(TMP^{+\bullet})Fe^{III}]$ (~1.1 V vs SCE). Sawyer et al. reported that the electrochemistry of the oxoiron(IV) 5,10,15,20-tetrakis(2,6-dichlorophenyl)porphyrin π-cation radical complex, $[(TDCP^{+\bullet})Fe^{IV}O]^+$, prepared by ozone oxidation in acetonitrile at −35 °C, showed a reversible redox peak at 1.27 V versus SCE.[7] This was assigned as the (TDCP)$Fe^{IV}O/[(TDCP^{+\bullet})Fe^{IV}O]^+$ couple. The absence of comprehensive studies of the redox potentials of oxoiron(IV) porphyrin π-cation radical complexes has hampered the identification of electron transfer processes in the reaction mechanisms.

In this article, we report a systematic low temperature study of the electrochemistry of oxoiron(IV) porphyrin and oxoiron(IV) porphyrin π-cation radical complexes having various porphyrin structures and axial ligands as shown in Figure 1. We assign redox potentials between oxoiron(IV) porphyrin and oxoiron(IV) porphyrin π-cation radical complexes, (P)$Fe^{IV}O/[(P^{+\bullet})Fe^{IV}O]^+$, using a combination of cyclic voltammograms and thin-layer spectroelectrochemistry. The redox potential for the (P)$Fe^{IV}O/[(P^{+\bullet})Fe^{IV}O]^+$ couple undergoes a positive shift upon coordination of an anionic axial ligand, but a negative shift upon coordination of a neutral axial ligand (imidazole). However, the electron-withdrawing effect of the meso-substituent shifts the redox potential in a positive direction. On the basis of the measured redox potentials, the participation of the electron transfer process from substrates to the oxoiron(IV) porphyrin π-cation radical complex in the oxygenation mechanism is discussed.

EXPERIMENTAL SECTION

Materials. Anhydrous dichloromethane was commercially obtained and stored in the presence of 4 Å molecular sieves. Other chemicals were commercially obtained and used without further purification. 5,10,15,20-Tetramesitylporphyrin (TMP), 5,10,15,20-tetrakis-pentafluorophenylporphyrin (TPFP), and 2,7,12,17-teramethyl-3,8,13,18- tetramesitylporphyrin (TMTMP) were prepared according to previously described methods.[32,33] (TMP)$Fe^{III}Cl$, (TPFP)$Fe^{III}Cl$, and (TMTMP)$Fe^{III}Cl$ were prepared by insertion of iron into porphyrins with $FeCl_2$ and sodium acetate in acetic acid and purified with a silica gel column using CH_2Cl_2/CH_3OH as an eluent.[8] (TMP)$Fe^{III}ClO_4$, (TPFP)$Fe^{III}ClO_4$, and (TMTMP)$Fe^{III}ClO_4$ were prepared by the reaction of iron(III) porphyrin chloride complexes with silver(I) perchlorate in dichloromethane solution and purified by recrystallization from dichloromethane/*n*-hexane.[34] (TMP)$Fe^{III}OH$ and (TMTMP)$Fe^{III}OH$ were obtained from (TMP)$Fe^{III}Cl$ and (TMTMP)$Fe^{III}Cl$ respectively by passing through a basic alumina (10% water) column using dichloromethane as an eluent.[35] Tetra-*n*-butylammonium 3-fluoro-4-nitrophenolate, *n*-Bu_4N(3-F-4-NO_2-PhO), was prepared from the reaction of tetra-*n*-butylammonium hydroxide and 3-fluoro4-nitrophenol and purified by recrystallization in dichloromethane-hexane.

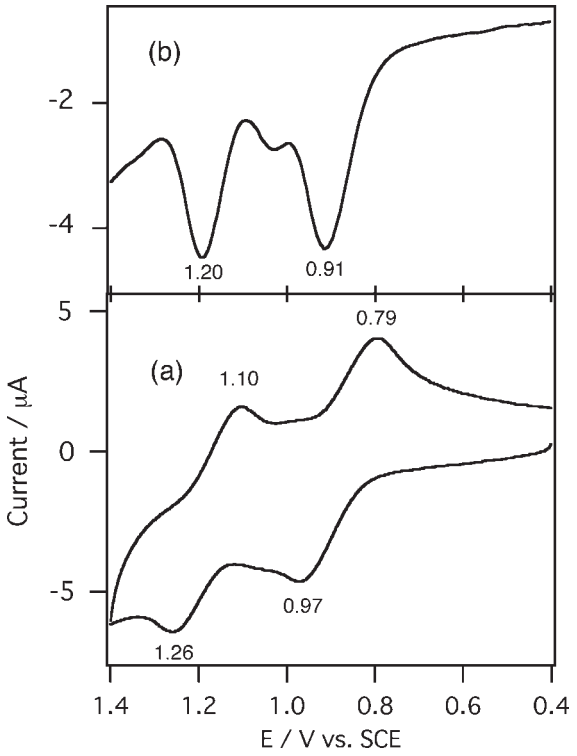

Figure 2. (a) Cyclic voltammogram and (b) differential pulse voltammogram of (TMP)$Fe^{IV}O$ in dichloromethane containing 0.1 M tetra-*n*-butylammonium perchlorate at −60 °C. The scan rate was 100 mV/s.

Preparation of Oxoiron(IV) Porphyrin Complexes. Oxoiron(IV) porphyrin complexes were prepared as previously described.[35] $(TMP^{+\bullet})Fe^{III}(ClO_4)_2$ or $(TMTMP^{+\bullet})Fe^{III}(ClO_4)_2$, which were prepared from oxidation of (TMP)$Fe^{III}OH$ or (TMTMP)$Fe^{III}OH$ by addition of solid ferric perchlorate in dichloromethane, was transferred through a short basic alumina (20% water) column (0.5 × 1 cm) at ambient temperature directly into an electrochemical cell containing anhydrous dichloromethane and 0.1 M *n*-Bu_4NClO_4, which was precooled in a temperature controlled cooling bath. For preparation of a series of imidazole complexes, 1 equiv of 1-MeIm, 2-MeIm, or 4(5)-MeIm was slowly added to the cooled solution. A series of complexes with anionic axial ligands was prepared by addition of 1 equiv of tetra-*n*-butylammonium salts, *n*-$Bu_4N(L)$, where L is fluoride, chloride, acetate, trifluoroacetate, benzoate, nitrate, and 3-fluoro-4-nitrophenolate.

Preparation of Oxoiron(IV) Porphyrin π-Cation Radical Complexes. Oxoiron(IV) porphyrin π-cation radical complexes were prepared by ozone oxidation at low temperature.[10,36] Iron(III) porphyrin complexes were dissolved in anhydrous solvent containing 0.1 M *n*-Bu_4NClO_4 in an electrochemical cell. The electrochemical cell was cooled in a temperature-controlled cooling bath. Ozone gas was slowly bubbled into the solution using a gastight syringe. With the formation of oxoiron(IV) porphyrin π-cation radical complexes, the brown solution changed to green. Excess ozone gas was removed by bubbling argon gas using a gastight syringe.

Instrumentation. UV−vis absorption spectra were recorded on an Agilent 8453 spectrometer (Agilent Technologies) equipped with a USP-203 low-temperature chamber (UNISOKU). Cyclic voltammogram (CV) and differential pulse voltammogram (DPV) were measured in a conventional three-electrode electrochemical cell with an ALS612A electrochemical analyzer. Tetra-*n*-butylammonium perchlorate, *n*-Bu_4NClO_4, (0.1 M) was used as a supporting electrolyte. The working electrode

dx.doi.org/10.1021/ic102564e |*Inorg. Chem.* 2011, 50, 6922–6928

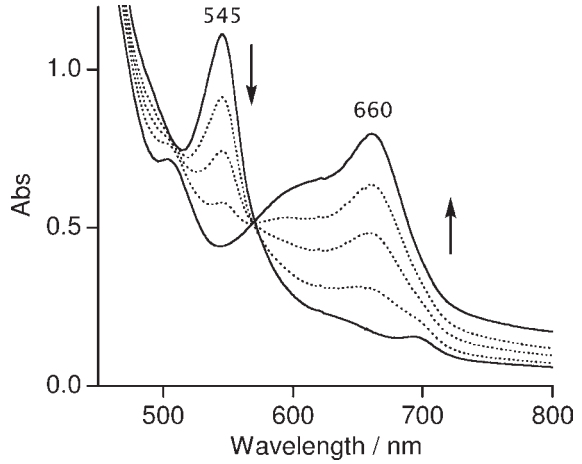

Figure 3. Absorption spectral change for electrochemical oxidation of (TMP)$Fe^{IV}O$ at 1.10 V vs SCE in dichloromethane containing 0.1 M tetra-*n*-butylammonium perchlorate at −60 °C. Experimental conditions are described in the Experimental Section.

was a glassy carbon electrode and the counter electrode was a platinum-wire electrode. The potentials were recorded with respect to a saturated calomel electrode (SCE) as a reference electrode. Temperature of electrochemical cell was controlled by a PSL-1800 low temperature cryostat bath (EYELA, Tokyo).

Spectroelectrochemistry. Spectroelectrochemsitry was carried out in a handmade thin-layer quartz cell (optical path = 0.5 mm) with a gold-mesh (100 mesh) working electrode, a platinum-wire counter electrode, and an Ag reference electrode (Figure S1 of the Supporting Information), which were connected to a HA-151 potentiostat-galvanostat (HOKUTO DENKO). The $E_{1/2}$ value of ferrocene in this spectroelectrochemical cell was 0.370 V at −40 °C, which was 0.100 V lower than that measured in the electrochemical cell with SCE reference electrode described above. Therefore, to apply the potential versus SCE, the applied potentials to the spectroelectrochemical cell were 100 mV lower than the desired potentials versus SCE. The spectroelectrochemical cell was placed in a low-temperature chamber set on a spectrometer and cooled to low temperature (213 or 193 K). Samples were prepared as described above. After bubbling Ar gas, a constant potential was applied while monitoring UV−vis absorption spectral changes.

■ RESULTS AND DISCUSSION

Electrochemistry. We measured the cyclic voltammogram (CV) of (TMP)$Fe^{IV}O$ in dichloromethane containing 0.1 M *n*-Bu_4NClO_4 at −60 °C. As shown in Figure 2, (TMP)$Fe^{IV}O$ exhibits two quasi-reversible redox waves at $E_{1/2}$ = 0.88 and 1.18 V versus SCE. The obtained CV was similar to the CV reported for (TDCP$^{+\bullet}$)$Fe^{IV}O(ClO_4)$ in acetonitrile at −35 °C,[7] except for ∼300 mV negative shifts of the redox peaks. The differential pulse voltammogram of (TMP)$Fe^{IV}O$ showed two peaks at 0.91 and 1.20 V versus SCE. The small peak at 1.03 V was due to a decomposed iron(III) porphyrin complex because the peak became strong with thermal decomposition of the sample. (TMP)$Fe^{IV}O$ did not show significant peaks from 0.5 V to −0.5 V versus SCE, but a strong catalytic current below −0.75 V, probably due to reductive decomposition of (TMP)$Fe^{IV}O$ (Figure S2 of the Supporting Information). To further confirm whether these peaks resulted from redox processes of (TMP)$Fe^{IV}O$, we measured the CV of (TMP$^{+\bullet}$)$Fe^{IV}O(ClO_4)$ in acetonitrile containing 0.1 M *n*-Bu_4NClO_4 at −35 °C. The result revealed a CV similar to that of (TMP)$Fe^{IV}O$ (Figure S3 of the Supporting Information). The first redox potential at $E_{1/2}$ = 0.88 V in acetonitrile was same as that in dichloromethane, but the second redox potential at $E_{1/2}$ = 1.25 V in acetonitrile was slightly higher than that in dichloromethane. This is most likely due to a solvent effect. Moreover, the CV was different from that of a thermally decomposed compound of (TMP$^{+\bullet}$)$Fe^{IV}O(ClO_4)$. These results indicate that these peaks result from redox processes of (TMP)$Fe^{IV}O$ and (TMP$^{+\bullet}$)$Fe^{IV}O(ClO_4)$.

To assign the redox potential for the (TMP)$Fe^{IV}O$/(TMP$^{+\bullet}$)$Fe^{IV}O(ClO_4)$ couple, we performed thin-layer spectroelectrochemistry for (TMP)$Fe^{IV}O$ in dichloromethane containing 0.1 M *n*-Bu_4NClO_4 at −60 °C. By applying 1.10 V versus SCE, the voltage between the first and second peaks, the absorption spectrum of (TMP)$Fe^{IV}O$ changed to that of (TMP$^{+\bullet}$)$Fe^{IV}O(ClO_4)$ with clear isosbestic points (Figure 3). This clearly indicates that the redox peaks at E_a = 0.79 and E_c = 0.97 V ($E_{1/2}$ = 0.88 V) correspond to the redox potential of the (TMP)$Fe^{IV}O$/[(TMP$^{+\bullet}$)$Fe^{IV}O$]$^+$ process.

As expected from the work of Balch et al,[31] the redox potential for the (TMP)$Fe^{IV}O$/[(TMP$^{+\bullet}$)$Fe^{IV}O$]$^+$ couple was unexpectedly low relative to that of (TMP)$Fe^{III}X$/[(TMP$^{+\bullet}$)-$Fe^{III}X$]$^+$ (∼1.1 V vs SCE). This is due to the strong electron donor effect of the oxo-ligand, which increases the electron density on the porphyrin ring via the ferryl iron. A similar effect of the oxo-ligand was also identified in the redox potentials of other oxo-metalloporphyrin complexes, such as (TMP)$Cr^{IV}O$ (0.76 V vs Ag/AgCl) and (TMP)$Ru^{VI}O_2$ (0.61 V vs Ag/AgCl).[37]

We also examined thin-layer spectroelectrochemistry for (TMP$^{+\bullet}$)$Fe^{IV}O(ClO_4)$ to assign the second redox process at −80 °C (Figure S4 of the Supporting Information). With applying 1.45 V versus SCE, the absorption spectrum of (TMP$^{+\bullet}$)$Fe^{IV}O(ClO_4)$ changed to a new one having Soret band at 368 nm and weak bands from 900 to 500 nm, and then a final one having absorption peaks at around 353 and 730 nm. The final compound was not reduced to (TMP$^{+\bullet}$)$Fe^{IV}O(ClO_4)$ even when 0.30 V versus SCE was applied. Moreover, the similar spectral change was observed when trifluoroacetic acid was titrated to (TMP$^{+\bullet}$)$Fe^{IV}O(NO_3)$ (data not shown). These results indicate that the final compound is not one-electron oxidized species of (TMP$^{+\bullet}$)$Fe^{IV}O(ClO_4)$ but probably its decomposed compound. The absorption spectrum of the final compound is unique and further spectroscopic studies are required to characterize it.

Porphyrin and Axial Ligand Effects. To investigate the effect of an anionic axial ligand on the redox potential of oxoiron(IV) porphyrin π-cation radical complex, we measured a series of CVs of (TMP)$Fe^{IV}O$ in the presence of 1 equiv of *n*-$Bu_4N(L)$, where L is fluoride, chloride, acetate, benzoate, trifluoroacetate, and nitrate. The CVs in the presence of *n*-$Bu_4N(L)$ were similar to those in the absence of *n*-$Bu_4N(L)$, but the redox peaks were shifted to the more positive region (Figure S5 of the Supporting Information). To assign these redox peaks, we examined the thin-layer spectroelectrochemistry of (TMP)$Fe^{IV}O$ in the presence of 1 equiv of *n*-Bu_4NF in dichloromethane containing 0.1 M *n*-Bu_4NClO_4 at −60 °C (Figure S6 of the Supporting Information). The absorption spectrum of (TMP)$Fe^{IV}O$ in the presence of 1 equiv of *n*-Bu_4NF was similar to that in the absence of *n*-Bu_4NF. By applying 1.20 V versus SCE, the absorption spectrum of (TMP)$Fe^{IV}O$ changed to that of (TMP$^{+\bullet}$)$Fe^{IV}O(F)$, indicating that the first redox peaks were due to the (TMP)$Fe^{IV}O$/[(TMP$^{+\bullet}$)$Fe^{IV}O$]$^+$ couple. In addition, these results indicate that fluoride ion binds as an axial ligand for [(TMP$^{+\bullet}$)$Fe^{IV}O$]$^+$, but the

dx.doi.org/10.1021/ic102564e |*Inorg. Chem.* 2011, 50, 6922–6928

Table 1. Redox Potentials (vs SCE[a]) of Iron(III) Porphyrin and Oxoiron(IV) Porphyrin π-Cation Radical Complexes in Dichloromethane at −60 °C

porphyrin	axial ligand (L)	first: (P)$Fe^{IV}O$/ ($P^{+\bullet}$)$Fe^{IV}O$[b]			second[b]	(P)Fe^{III}/ ($P^{+\bullet}$)Fe^{III}[b]	ref
		E_{pa}	E_{pc}	$E_{1/2}$	$E_{1/2}$	$E_{1/2}$	
TMP	perchlorate	0.97	0.79	0.88 (0.91)	1.18 (1.20)	1.09 (1.08)	
	perchlorate [c]	0.91	0.84	0.88 (0.90)	1.25 (1.28)	1.12(1.15)	
	fluoride	1.03	0.89	0.96 (0.95)	1.25 (1.22)	1.10 (1.09)	
	chloride	1.06	0.88	0.97 (0.94)	1.26 (1.23)	1.10 (1.04)	
	acetate	1.10	0.89	1.04 (1.04)	1.26 (1.24)	1.06 (1.03)	
	trifluoroacetate	1.02	0.90	0.96 (0.96)	1.25 (1.22)	1.09 (1.08)	
	benzoate	1.09	0.89	0.99 (1.04)	1.25 (1.23)	1.05	
	nitrate	1.03	0.88	0.95 (0.94)	1.21 (1.19)	1.11	
	3-fluoro-4-nitrophenolate	1.03	0.89	0.96 (0.96)	1.25 (1.23)	1.16	
	imidazole	0.84	0.76	0.80 (0.76)	1.01 (0.98)	nd	
	2-methylimidazole	0.81	0.73	0.77 (0.75)	1.02 (1.00)	nd	
	5-methylimidazole	0.78	0.73	0.76 (0.72)	0.98 0.96)	nd	
TDCP	perchlorate[c]	1.30	1.25	1.275	1.59	~1.46	7
TPFP	perchlorate[d]	1.43	1.35	1.39 (1.39)	nd	(1.56)	
TMTMP	perchlorate	0.98	0.83	0.90 (0.92)	1.22 (1.19)	1.07(1.06)	
	nitrate	1.01	0.89	0.95 (0.94)	1.30 (1.28)	1.09(1.08)	
	imidazole	0.87	0.80	0.84	0.99	nd	

[a] In our system, the redox potential ($E_{1/2}$) of ferrocene was 0.460 V at −60 °C and 0.528 V at 20 °C. [b] Values in parentheses were obtained from differential pulse voltammetry. [c] In acetonitrile at −35 °C. [d] In dichloromethane/acetonitrile (1:1).

binding of fluoride ion is not sure for (TMP)$Fe^{IV}O$. To study the binding ability of anionic ligands to (TMP)$Fe^{IV}O$, (TMP)$Fe^{IV}O$ was titrated with *n*-Bu_4N(L), where L is fluoride, chloride, and benzoate, at −60 °C (Figure S7 of the Supporting Information). With increase in amount of fluoride ion, the absorption at 545 nm for (TMP)$Fe^{IV}O$ slightly decreased its intensity and shifted to 554 nm. The peak intensity was also decreased with addition of chloride and benzoate, but the peak did not shift even with addition of excess amount. These results indicated that anionic ligands bind with (TMP)$Fe^{IV}O$, but their affinities seems to be low. The $E_{1/2}$ values for the (TMP)Fe^{IV}O(L)/($TMP^{+\bullet}$)Fe^{IV}O(L) couple are summarized in Table 1. Interestingly, the redox potential showed a positive shift upon coordination of the anionic axial ligand but was not changed significantly by the identity of the axial ligand. This is the same as the redox potential for (TMP)Fe^{III}X/[($TMP^{+\bullet}$)Fe^{III}X]$^+$, and the insensitivity of the redox potential to the axial anion would be due to that the redox process occurs at porphyrin macrocycle but not iron center.

We also examined CVs of a series of ($TMP^{+\bullet}$)Fe^{IV}O(L) complexes. However, ($TMP^{+\bullet}$)Fe^{IV}O(L) could not be formed from (TMP)Fe^{III}(L) in acetonitrile at −40 °C by ozone oxidation when L is other than perchlorate. ($TMP^{+\bullet}$)Fe^{IV}O(L) were prepared and measured CVs in dichloromethane containing 0.1 M *n*-Bu_4NClO_4 at −60 °C (Figure S8 of the Supporting Information). The CVs of ($TMP^{+\bullet}$)Fe^{IV}O(L) were different from those of (TMP)$Fe^{IV}O$ in the presence of 1 equiv of *n*-Bu_4N(L). ($TMP^{+\bullet}$)Fe^{IV}O(L) exhibited quasi-reversible redox peaks at around 1.0 V, but the $E_{1/2}$ values of the redox peaks were different from those of (TMP)$Fe^{IV}O$. Moreover, irreversible peaks were observed at around 0.6 V versus SCE. The complicated CVs of ($TMP^{+\bullet}$)Fe^{IV}O(L) do not seem to show redox potential for (TMP)$Fe^{IV}O$/($TMP^{+\bullet}$)Fe^{IV}O(L) couple correctly. These differences would be induced by contamination of hydrochloric acid, which is formed from the ozone-driven oxidation of dichloromethane. The decomposition of unstable ($TMP^{+\bullet}$)-Fe^{IV}O(L) and participation of proton in the redox processes make assignments of these redox peaks difficult.

Imidazole and phenolate are the axial ligands of peroxidases and catalases, respectively. To investigate the axial ligand effects of imidazole and phenolate, we measured CVs of (TMP)$Fe^{IV}O$ in the presence of 1 equiv of imidazole, 2-methylimidazole, 5-methylimidazole, and *n*-Bu_4N(3-F-4-NO_2−PhO) (part f of Figure S5, and Figure S9 of the Supporting Information). The CV of (TMP)Fe^{IV}O(Im) was very close to that of (TMP)$Fe^{IV}O$, but the redox potential for (TMP)Fe^{IV}O(Im)/[($TMP^{+\bullet}$)Fe^{IV}-O(Im)]$^+$ was found to be lower than that of (TMP)-Fe^{IV}O/[($TMP^{+\bullet}$)Fe^{IV}O]$^+$ (Table 1). (TMP)Fe^{IV}O(2-MeIm) and (TMP)Fe^{IV}O(5-MeIm) were found to exhibit similar CVs and the redox potential was increased in the order of 5-MeIm < 2-MeIm < Im < none. The redox potentials (0.76−0.80 V vs SCE) for these imidazole complexes were in the range of redox potentials reported for compound II/compound I of peroxidases (0.66−0.91 V vs SCE).[23−30] However, the redox potential for the 3-fluoro-4-nitrophenolate complex was higher than that for (TMP)$Fe^{IV}O$ and close to those of the other anionic ligands.

In a previous article, we showed that the reactivity of the oxoiron(IV) porphyrin π-cation radical complex for cyclooctene epoxidation is drastically changed by the axial ligand and increases in the order of nitrate < chloride < 3-fluoro-4-nitrophenolate ≤ imidazole.[8b] This study clearly showed that the redox potentials of these complexes do not match this reactivity order. This indicates that the axial ligand effect on the reactivity of oxoiron(IV) porphyrin π-cation radical complex cannot be rationalized by the change of the redox potential. In fact, as discussed in later section, the direct electron transfer process from cyclooctene to oxoiron(IV) porphyrin π-cation radical complex may not be involved in its rate-limiting step. The axial ligand modulates reactivity of oxoiron(IV) porphyrin π-cation

dx.doi.org/10.1021/ic102564e |*Inorg. Chem.* 2011, 50, 6922–6928

radical complex by changing other factors than its redox potential. The axial ligand effect must be further studied from various spectroscopic methods.

Electron-withdrawing porphyrin substituents have been shown to increase the oxygenation reactivity of the oxoiron(IV) porphyrin π-cation radical complex.[8a,38] We measured the redox potential of $(TPFP^{+\bullet})Fe^{IV}O(ClO_4)$ in dichloromethane/acetonitrile at −60 °C. The CV of $(TPFP^{+\bullet})Fe^{IV}O(ClO_4)$ was found to be similar to that of $(TMP^{+\bullet})Fe^{IV}O(ClO_4)$, but the redox peaks showed significant positive shifts. The $E_{1/2}$ for $(TPFP)Fe^{IV}O/[(TPFP^{+\bullet})Fe^{IV}O]^+$ is 1.39 V versus SCE. This is 510 mV higher than that of $(TMP^{+\bullet})Fe^{IV}O(ClO_4)$. It is clear that the $E_{1/2}$ value for the $(P)Fe^{IV}O/[(P^{+\bullet})Fe^{IV}O]^+$ couple increases with an increase in the electron-withdrawing effect of the meso substituent.

We measured CVs of $(TMTMP)Fe^{IV}O$, which has mesityl groups at the pyrrole β-position, to compare the redox potentials of $(TMP)Fe^{IV}O$ (Figure S10 of the Supporting Information). Previously, we showed that the porphyrin π-cation radical of $(TMTMP^{+\bullet})Fe^{IV}O$ is in the a_{1u} orbital, whereas that of $(TMP^{+\bullet})Fe^{IV}O$ is in the a_{2u} orbital.[8a] The data obtained from the CV of $(TMTMP)Fe^{IV}O$ are listed in Table 1. In spite of the radical occupying different porphyrin π-cation orbitals, the redox potentials of $(TMTMP)Fe^{IV}O$ were found to be close to that of $(TMP)Fe^{IV}O$. This was also observed for the nitrate and imidazole complexes.

Electron Transfer in the Reaction Mechanism. The redox potentials of oxoiron(IV) porphyrin π-cation radical complexes provide useful information for discussions of the participation of electron transfer processes in oxygenation mechanisms. Epoxidations of olefins are one of the best studied reactions for oxoiron(IV) porphyrin π-cation radical complexes and there have been several reaction intermediates proposed.[15−19] Here, we discuss the participation of electron transfer processes in an epoxidation mechanism with the measured redox potentials and the reaction rate constants for epoxidation of cyclooctene with $(TMP^{+\bullet})Fe^{IV}O(L)$.[8b] The free energy of activation ($\Delta G^{\ddagger}_{CO}$) for cyclooctene epoxidation calculated from Eyring's equation, $\Delta G^{\ddagger} = -RT\ln k_2h/kT$ (where R is the gas constant, k_2 is reaction rate constant, h is the Plank constant, k is Boltzmann constant, and T is temperature) is approximately 60 kJ/mol at 213 K when L is nitrate ($k_2 = 8.21 \times 10^{-4}$ $M^{-1}s^{-1}$). A similar value was obtained when $\Delta G^{\ddagger}$ values were calculated from the enthalpy of activation ($\Delta H^{\ddagger}$) and entropy of activation ($\Delta S^{\ddagger}$), estimated from an Eyring plot (data not shown). However, the change of free energy (ΔG°_{ET}) for the electron transfer from cyclooctene to $(TMP^{+\bullet})Fe^{IV}O(L)$ is calculated to be ∼100 kJ/mol from the relationship, $\Delta G^{\circ} = nF(P_1 - P_2)$, where n is number of electrons ($n = 1$), F is Faraday's constant, P_1 is the redox potential of cyclooctene (2.03 V vs SCE),[39] and P_2 is the redox potential of $(TMP^{+\bullet})Fe^{IV}O(L)$ (0.95 V vs SCE for L = nitrate). Obviously, the $\Delta G^{\ddagger}$ value is much smaller than the ΔG° value. Therefore, the results of these calculations enable us to rule out direct electron transfer from cyclooctene to $(TMP^{+\bullet})Fe^{IV}O(L)$ in the reaction mechanism of cyclooctene epoxidation. As previously suggested for epoxidation by the oxochromium(V) porphyrin complex,[39,40] weak orbital interactions between cyclooctene and the Fe═O moiety of the oxoiron(IV) porphyrin π-cation radical complex may be formed at the transition state and the electron transfer may occur in the bond formation process between the oxo-ligand of Fe═O and C═C moiety of cyclooctene (Figure 4).

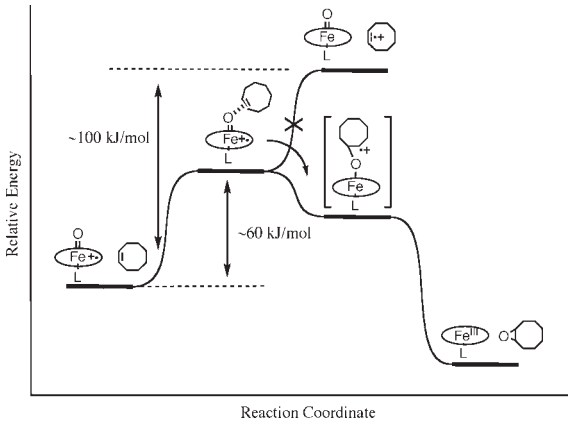

Figure 4. Reaction coordinate diagram showing the reaction profile for the epoxidation reaction of cyclooctene by $(TMP^{+\bullet})Fe^{IV}O(L)$. The values are for nitrate complex. The relative energies of bond-formation complex and the final product are uncertain.

The reaction mechanisms of amine *N*-demethylation catalyzed by heme-containing peroxidases and cytochrome P450 have been studied over the past four decades.[14,41−48] The mechanisms were also studied with synthetic model complexes.[49−52] Whereas the overall reaction consists of hydroxylation of the *N*-methyl group followed by hydrolysis to afford *N*-demethylated amine and formaldehyde, the mechanism of the hydroxylation remains controversial. These enzymatic and model studies proposed two different mechanisms: a hydrogen atom transfer (HAT) mechanism and consecutive electron-transfer proton-transfer (ET/PT) mechanism. Previous studies of catalytic demethylation reactions with iron(III) porphyrins supported ET/PT mechanism.[49,50] The demethylation reaction by $(TMP^{+\bullet})Fe^{IV}O(L)$ was proposed to proceed via electron transfer followed by H-atom transfer, which competes with back electron transfer.[14] To further investigate the reaction mechanism of the demethylation reaction of aniline with the oxoiron(IV) porphyrin π-cation radical complex, we calculated the change of free energies (ΔG°_{ET}) for the electron transfer from *p*-substituted *N*,*N*-dimethylanilines to $(TMP^{+\bullet})Fe^{IV}O(L)$ using the relationship $\Delta G^{\circ} = nF(P_1 - P_2)$ and the free energies of activation ($\Delta G^{\ddagger}_{DMA}$) for these demethylation reactions at 220 K using Eyring's equation. The calculated energies are summarized in Figure 5. When the substrate is *N*,*N*-dimethyl-*p*-nitroaniline, which has a strong electron-withdrawing substituent and high oxidation potential ($E_{1/2}$ = 1.38 V vs SCE),[14] the ΔG°_{ET} value is calculated to be +38 kJ/mol. Therefore, the direct electron transfer process from *N*,*N*-dimethyl-*p*-nitroaniline to $(TMP^{+\bullet})Fe^{IV}O(L)$ is energetically uphill. The ΔG°_{ET} value is smaller than the $\Delta G^{\ddagger}_{N\text{-}DMA}$ value (∼49 kJ/mol) calculated from Eyring's equation with $k_2 = 2.2 \times 10$ M^{-1} s^{-1} at 223 K.[14] Moreover, previous study showed large kinetic isotope effect and agreement of kinetic and product isotope effects for *N*,*N*-dimethyl-*p*-nitroaniline.[14] These results clearly indicate that the H-atom transfer step from the methyl group of the formed amine radical would be the rate-limiting step of the overall reaction and the electron transfer process may occur before the H-atom transfer. The energy barrier for the H-atom transfer process can be estimated to be ∼11 kJ/mol. Back electron transfer easily occur because the activation energy for the back electron transfer process is smaller than that for the subsequent H-atom transfer process from the methyl group of the formed amine radical

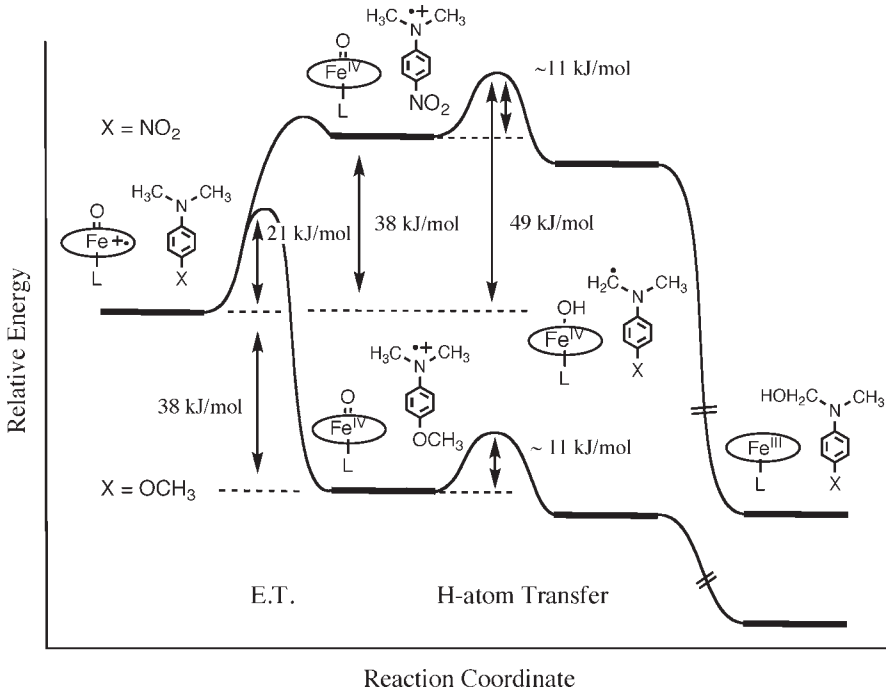

Figure 5. Reaction coordinate diagram showing the reaction profile for the demethylation of *N*,*N*-dimethyl-*p*-nitroaniline and *N*,*N*-dimethyl-*p*-methoxyaniline with $(TMP^{+\bullet})Fe^{IV}O(L)$. The structure of the H-atom transferred complex and the relative energies of the H-atom transferred complex and the final products are uncertain.

(Figure 5). However, when the substrate is *N*,*N*-dimethyl-*p*-methoxyaniline, which has a strong electron-donating substituent and low oxidation potential ($E_{1/2}$ = 0.60 V vs SCE),[14] the calculated ΔG°_{ET} value (−38 kJ/mol) was also found to be much smaller than the $\Delta G^{\ddagger}_{M\text{-}DMA}$ value (21.0 kJ/mol) calculated from Eyring's equation with $k_2 = 5.6 \times 10^7\ M^{-1}s^{-1}$ at 223 K.[14] The direct electron transfer process from *N*,*N*-dimethyl-*p*-methoxyaniline to $(TMP^{+\bullet})Fe^{IV}O(L)$ is energetically downhill. The energy barrier of the following H-atom transfer process for *N*,*N*-dimethyl-*p*-methoxyaniline may be close that (~11 kJ/mol) for *N*,*N*-dimethyl-*p*-nitroaniline. These results indicate that the first electron transfer step becomes the rate-limiting step of the overall reaction (Figure 5). This is also consistent to a very small kinetic isotope effect for *N*,*N*-dimethyl-*p*-methoxyaniline, as previously reported.[14] The transition state of the rate-limiting step would be the formation of the complex between $(TMP^{+\bullet})Fe^{IV}O(L)$ and *N*,*N*-dimethyl-*p*-methoxyaniline for electron transfer. Back electron transfer is prevented from occurring because the activation energy for the subsequent H-atom transfer from the methyl group of the formed amine radical is lower than the activation energy for the back electron transfer (Figure 5). Finally, it is obvious that the stability of the electron transferred complex, which is determined by the difference of the redox potential between oxoiron(IV) porphyrin π-cation radical complex and *N*,*N*-dimethylaniline, controls the character of the rate-limiting step.

In summary, we reported herein electrochemistry of oxoiron(IV) porphyrin and oxoiron(IV) porphyrin π-cation radical complexes having various porphyrin structures and axial ligands in organic solvents at low temperatures. The redox potential for the $(TMP)Fe^{IV}O/[(TMP^{+\bullet})Fe^{IV}O]^+$ couple was observed at 0.88 V versus SCE, which showed a positive shift upon coordination of an anionic axial ligand but a negative shift upon coordination of imidazole. The electron-withdrawing effect of the meso-substituent shifts the redox potential in a positive direction. The measured redox potentials in this study provide useful information to analyze electron transfer processes in oxygenation mechanisms of various organic substrates. The direct electron transfer process from cyclooctene to $(TMP^{+\bullet})Fe^{IV}O(L)$ is not involved in the reaction mechanism of cyclooctene epoxidation. On the other hand, demethylation reaction of *N*,*N*-dimethylanilines may proceed via electron transfer process followed by H-atom transfer. The rate-limiting step is the electron transfer process from aniline to oxoiron(IV) porphyrin π-cation radical for electron-rich aniline, but is the H-atom transfer process from the methyl group of the formed amine radical for electron-deficient aniline.

■ ASSOCIATED CONTENT

Supporting Information. Scheme of spectroelectrochemical cell, cyclic voltammograms of $(TMP)Fe^{IV}O(L)$ and $(TMP^{+\bullet})Fe^{IV}O(L)$, spectroelectrochemistry of $(TMP^{+\bullet})Fe^{IV}O(ClO_4)$ and $(TMP)Fe^{IV}O$ in the presence of 1 equiv of *n*-Bu_4NF, and titration of $(TMP)Fe^{IV}O$ with *n*-$Bu_4N(L)$. This material is available free of charge via the Internet at http://pubs.acs.org.

■ AUTHOR INFORMATION

Corresponding Author
*E-mail: hiro@ims.ac.jp.

■ ACKNOWLEDGMENT

This study was supported by grants from JSPS (Grant-in-Aid for Science Research, Grant No. 22350030), JST (CREST), and MEXT (Global COE Program).

REFERENCES

(1) Schonbaum, G. R.; Chance, B. In *The Enzymes*; Boyer, P. D., Ed.; Academic Press: New York, 1976; Vol. 13, pp 363−408.

(2) (a) Dunford, H. B. *Heme Peroxidases*; Wiley-VCH: New York, 1999. (b) Dunford, H. B.; Stillman, J. S. *Coord. Chem.* **1976**, *19*, 187–251.

(3) (a) Watanabe, Y.; Groves, J. T. In *The Enzymes*; Sigman, D. S., Ed.; Academic Press: New York, 1992; Vol. 20, pp 405−452. (b) Watanabe, Y.; Fujii, H. In *Struct. Bonding (Berlin)*; Meunier, B., Ed.; Springer: Berlin, 2000; Vol. 97, pp 61−89.

(4) Oritz de Montellano, P. R. In *Cytochrome P450: Structure, Mechanism, and Biochemistry*, 2nd ed.; Plenum Publishing Corporation: New York, 1995.

(5) (a) Dawson, J. H.; Sono, M. *Chem. Rev.* **1987**, *87*, 1255–1276. (b) Fujii, H. *Coord. Chem.* **2002**, *226*, 51–60.

(6) Groves, J. T.; Haushalter, R. C.; Nakamura, M.; Nemo, T. E.; Evans, B. J. *J. Am. Chem. Soc.* **1981**, *103*, 2884–2886.

(7) Sugimoto, H.; Tung, H.; Sawyer, D. H. *J. Am. Chem. Soc.* **1988**, *110*, 2465–2470.

(8) (a) Fujii, H. *J. Am. Chem. Soc.* **1993**, *115*, 4641–4648. (b) Takahashi, A.; Kurahashi, T; Fujii, H. *Inorg. Chem.* **2009**, *48*, 2614–2625.

(9) Song, W. J.; Ryu, Y. O.; Song, R.; Nam, W. *J. Biol. Inorg. Chem.* **2005**, *10*, 294–304.

(10) (a) Gross, Z.; Nimri, S. *Inorg. Chem.* **1994**, *33*, 1731–1732. (b) Gross, Z.; Nimri, S.; Barzilay, C. M.; Simkhovich, L. *J. Biol. Inorg. Chem.* **1997**, *2*, 492–506.

(11) (a) Pan, Z.; Zhang, R.; Newcomb, M. *J. Inorg. Biochem.* **2006**, *100*, 524–532. (b) Zhang, R.; Nagraj, N.; Lansakara-P., D. S. P.; Hager, L. P.; Newcomb, M. *Org. Lett.* **2006**, *8*, 2731–2734. (c) Pan, Z.; Zhang, R.; Fung, L. W.-M.; Newcomb, M. *Inorg. Chem.* **2007**, *46*, 1517–1519.

(12) Kang, M.-J.; Song, W. J.; Han, A.-R.; Choi, Y. S.; Jang, H. G.; Nam, W. *J. Org. Chem.* **2007**, *72*, 6301–6304.

(13) Goto, Y.; Matsui, T.; Ozaki, S.; Watanabe, Y.; Fukuzumi, S. *J. Am. Chem. Soc.* **1999**, *121*, 9497–9502.

(14) Goto, Y.; Watanabe, Y.; Fukuzumi, S.; Jones, J. P.; Dinnocenzo, J. P. *J. Am. Chem. Soc.* **1998**, *120*, 10762–10763.

(15) (a) Groves, J. T.; Myers, R. S. *J. Am. Chem. Soc.* **1983**, *105*, 5791–5796. (b) Groves, J. T.; Nemo, T. *J. Am. Chem. Soc.* **1983**, *105*, 5786–5791. (c) Groves, J. T.; Subramanian, D. V. *J. Am. Chem. Soc.* **1984**, *106*, 2177–2181. (d) Groves, J. T.; Watanabe, Y. *J. Am. Chem. Soc.* **1986**, *108*, 507–508.

(16) (a) Traylor, T. G.; Xu, F. *J. Am. Chem. Soc.* **1988**, *110*, 1953–1958. (b) Traylor, T. G.; Nakano, T.; Dunlap, B. E.; Traylor, P. S.; Dolphin, D. *J. Am. Chem. Soc.* **1986**, *108*, 2782–2784. (c) Traylor, T. G.; Nakano, T.; Mikzstal, A. R.; Dunlap, B. E. *J. Am. Chem. Soc.* **1987**, *109*, 3625–3632.

(17) (a) Collman, J. P.; Brauman, J. I.; Meunier, B.; Rayback, S. A.; Kodadek, T. *Proc. Natl. Acad. Sci. U.S.A.* **1984**, *81*, 3245–3248. (b) Collman, J. P.; Brauman, J. I.; Meunier, B.; Hayashi, T.; Kodadek, T.; Rayback, S. A. *J. Am. Chem. Soc.* **1985**, *107*, 2000–2005. (c) Collman, J. P.; Kodadek, T.; Rayback, S. A.; Brauman, J. I.; Papazian, L. M. *J. Am. Chem. Soc.* **1985**, *107*, 4343–4345.

(18) (a) He, G.-X.; Arasasingham, R. D.; Zhang, G.; Bruice, T. C. *J. Am. Chem. Soc.* **1991**, *113*, 9828–9833. (b) Castellino, A. J.; Bruice, T. C. *J. Am. Chem. Soc.* **1988**, *110*, 158–162. (c) Castellino, A. J.; Bruice, T. C. *J. Am. Chem. Soc.* **1988**, *110*, 7512–7519.

(19) Gross, Z.; Nimri, S. *J. Am. Chem. Soc.* **1995**, *117*, 8021–8022.

(20) (a) Shaik, S.; Kumar, D.; de Visser, S. P.; Altun, A.; Thiel, W. *Chem. Rev.* **2005**, *105*, 2279–2328. (b) Shaik, S.; Kumar, D.; de Visser, S. P. *J. Am. Chem. Soc.* **2008**, *130*, 10128–10140.

(21) Korzekwa, K. R.; Jones, J. P.; Gillette, J. R. *J. Am. Chem. Soc.* **1990**, *112*, 7042–7046.

(22) Kamachi, T.; Yoshizawa, K. *J. Am. Chem. Soc.* **2003**, *125*, 4652–4661.

(23) Hayashi, Y.; Yamazaki, I. *J. Biol. Chem.* **1979**, *254*, 9101–9106.

(24) He, B.; Sinclair, R.; Copeland, B. R.; Powers, L. S. *Biochemistry* **1996**, *35*, 2413–2420.

(25) Farhangrazi, Z. S.; Fossett, M. E.; Powers, L. S.; Ellis, W. R. *Biochemistry* **1995**, *34*, 2866–2871.

(26) Torimura, M.; Mochizuki, M.; Kano, K.; Ikeda, T.; Ueda, T. *Anal. Chem.* **1998**, *70*, 4690–4695.

(27) Mondal, M. S.; Fuller, H. A.; Armstrong, F. A. *J. Am. Chem. Soc.* **1996**, *118*, 263–264.

(28) Arnold, J.; Furtmuller, P. G.; Regelsberger, G.; Obinger, C. *Eur. J. Biochem.* **2001**, *268*, 5142–5148.

(29) Furtmuller, P. G.; Arnold, J.; Jantschko, W.; Zederbauer, M.; Jakopitsch, C.; Obinger, C. *J. Inorg. Biochem.* **2005**, *99*, 1220–1229.

(30) Efimov, I.; Papadopoulou, N. D.; Mclean, K. J.; Badyal, S. K.; Macdonald, I. K.; Munro, A. W.; Moody, P. C. E.; Ravan, E. L. *Biochemistry* **2007**, *46*, 8017–8023.

(31) Balch, A. L.; Latos-Grazynski, L.; Renner, M W. *J. Am. Chem. Soc.* **1985**, *107*, 2983–2985.

(32) Lindsey, J.; Wagner, R. *J. Org. Chem.* **1989**, *54*, 828–836.

(33) Ono, N.; Kawamura, H.; Bougauchi, M.; Maruyama, K. *Tetrahedron* **1990**, *46*, 7483–7496.

(34) Reed, C. A.; Mashiko, T.; Bentley, S. P.; Kastner, M. E.; Scheidt, W. R.; Sparalian, K.; Lang, G. *J. Am. Chem. Soc.* **1979**, *101*, 2948–2958.

(35) Groves, J. T.; Gross, Z.; Stern, M. *Inorg. Chem.* **1994**, *33*, 5065–5072.

(36) Fujii, H.; Yoshimura, T.; Kamada, H. *Inorg. Chem.* **1997**, *36*, 6142–6143.

(37) Fujii, H.; Kurahashi, T.; Tosha, T.; Yoshimura, T.; Kitagawa, T. *J. Inorg. Biochem.* **2006**, *100*, 533–541.

(38) Fujii, H. *Chem. Lett.* **1994**, 1491–1494.

(39) Garrison, J. M.; Ostovic, D.; Bruice, T. C. *J. Am. Chem. Soc.* **1989**, *111*, 4960–4966.

(40) Garrison, J. M.; Bruice, T. C. *J. Am. Chem. Soc.* **1989**, *111*, 191–198.

(41) (a) Miwa, G. T.; Garland, W. A.; Hodshon, B. J.; Lu, A. Y.; Northrop, D. B. *J. Biol. Chem.* **1980**, *255*, 6049–6054. (b) Miwa, G. T.; Walsh, J. S.; Kedderis, G. L.; Hollenberg, P. F. *J. Biol. Chem.* **1983**, *258*, 14445–14449.

(42)(a) Guengerich, F. P.; Yun, C.-H.; Macdonald, T. L. *J. Biol. Chem.* **1996**, *271*, 27321–27329. (b) Okazaki, O.; Guengerich, F. P. *J. Biol. Chem.* **1993**, *268*, 1546–1552. (c) Macdonald, T. L.; Gutheim, W. G.; Martin, R. B.; Guengerich, F. P. *Biochemistry* **1989**, *28*, 2071–2077.

(43) Griffin, B. W.; Ting, P. L. *Biochemistry* **1978**, *17*, 2206–2211.

(44) Van der Zee, J.; Duling, D. R.; Mason, R. P.; Eling, T. E. *J. Biol. Chem.* **1989**, *264*, 19828–19836.

(45) (a) Kedderis, G. L.; Hollenberg, P. F. *J. Biol. Chem.* **1983**, *258*, 8129–8138. (b) Kedderis, G. L.; Koop, D. R.; Hollenberg, P. F. *J. Biol. Chem.* **1980**, *255*, 10174–10182.

(46) Lindsey Smith, J. R.; Mortimer, D. N. *J. Chem. Soc., Perkin Trans. 2* **1989**, 1743–1749.

(47) Manchester, J. I.; Dinnocenzo, J. P.; Higgins, L.; Jones, J. P. *J. Am. Chem. Soc.* **1997**, *119*, 5069–5070.

(48) Karki, S. B.; Dinnocenzo, J. P.; Jones, J. P.; Korzekwa, K. R. *J. Am. Chem. Soc.* **1995**, *117*, 3657–3664.

(49) Lindsay Smith, J. R.; Mortimer, D. N. *J. Chem. Soc., Perkin Trans. 2* **1986**, 1743–1749.

(50) Baciocchi, E.; Lanzalunga, O.; Lapi, A.; Manduchi, L. *J. Am. Chem. Soc.* **1998**, *120*, 5783–5787.

(51) Shearer, J.; Zhang, C. X.; Zakharov, L. N.; Rheingold, A. L.; Karlin, K. D. *J. Am. Chem. Soc.* **2005**, *127*, 5469–5483.

(52) Nehru, K.; Seo, M. S.; Kim, J.; Nam, W. *Inorg. Chem.* **2007**, *46*, 293–298.

NOTE ADDED AFTER ASAP PUBLICATION

This paper was published on the Web on June 29, 2011, with minor text errors. The corrected version was reposted on July 1, 2011.